AIIM

Association for Information and Image Management

1100 Wayne Avenue, Suite 1100
Silver Spring, Maryland 20910

301/587-8202

Centimeter

Inches

MANUFACTURED TO AIIM STANDARDS
BY APPLIED IMAGE, INC.

1 of 1

The submitted manuscript has been authored by a contractor of the U. S. Government under contract No. W-31-109-ENG-38. Accordingly, the U. S. Government retains a nonexclusive, royalty-free license to publish or reproduce the published form of this contribution, or allow others to do so, for U. S. Government purposes.

ILL-(TH)-94-2
FEB/94

ANL-HEP-TR-93-115

Quenched QCD at finite density

J. B. Kogut , M.-P. Lombardo

Physics Department, University of Illinois at Urbana-Champaign, Urbana, IL 61801-3080

D. K. Sinclair

HEP Division, Argonne National Laboratory, 9700 South Cass Avenue, Argonne, IL 60439

(January 31, 1994)

Abstract

Simulations of quenched QCD at relatively small but *nonzero* chemical potential μ on 32×16^3 lattices indicate that the nucleon screening mass decreases linearly as μ increases predicting a critical chemical potential of one third the nucleon mass, $m_N/3$, by extrapolation. The meson spectrum does not change as μ increases over the same range, from zero to $m_\pi/2$. Past studies of quenched lattice QCD have suggested that there is phase transition at $\mu = m_\pi/2$. We provide alternative explanations for these results, and find a number of technical reasons why standard lattice simulation techniques suffer from greatly enhanced fluctuations and finite size effects for μ ranging from $m_\pi/2$ to $m_N/3$. We find evidence for such problems in our simulations, and suggest that they can be surmounted by improved measurement techniques.

12.38.Mh, 12.38.Gc, 11.15.Ha

*Work supported by the U.S. Department of Energy, Division of High Energy Physics, Contract W-31-109-ENG-38.

MASTER

DISTRIBUTION OF THIS DOCUMENT IS UNLIMITED

Typeset using REVTEX

P-94-02-013

I. INTRODUCTORY COMMENTS

The search for the quark gluon plasma (QGP) is one of the major challenges posed by QCD, both theoretically and experimentally [1]. At the experimental level, no compelling evidence of this new state of matter has yet been found. Results are expected, however, from the experiments at RHIC. Most of the underlying physics of the QGP can be studied theoretically and computationally only by lattice simulations [2] [3] at this time. These have been quite successful in describing the physics at zero density and finite temperature, while simulations at finite density and zero temperature have been plagued in the past by many uncertainties [4].

First, simulations of QCD with virtual quarks are difficult because the action is complex at nonzero μ, thus preventing the naïve use of probabilistic methods in the evaluation of functional integrals. Nonetheless, complex Langevin simulations of spin models which are related to the strong coupling limit of lattice QCD have been quite encouraging [5]. We will see below that complex Langevin simulations of lattice QCD will, however, face numerical and conceptual problems which are not contained in toy spin models.

Second, while quark models of nuclear matter predict that the nucleon screening mass will decrease linearly with increasing chemical potential μ and a chiral symmetry restoring transition will occur at $\mu_c = m_N/3$ where the nucleon becomes massless, past simulations of the *quenched* theory have suggested that, in the limit of massless quarks, the system is in the deconfined, chirally symmetric phase no matter how small the chemical potential μ is [4]! When massive quarks have been simulated, the results have suggested that the critical chemical potential is $m_\pi/2$. This has caused most workers in the field to claim that quenched QCD is unphysical at nonzero μ. However, as we will discuss more fully below, there are several explanations for this apparently pathological behaviour which are unrelated to quenching: for instance, confinement is essential to obtain the correct μ dependence in QCD, but it is a property of the ensemble average of configurations, and need not be apparent configuration by configuration; the lattice spacing used in the simulations has been too

coarse, and, as a consequence, flavor symmetry breaking caused by staggered fermions may play an important role and suppress one's estimate of μ_c [6]; finite volume effects are very large at finite μ [7]; and, quark propagator algorithms are very slowly convergent at nonzero μ [2].

Attempts to clarify these issues by studying simpler models have not been decisive. Although the quenched approximation failed qualitatively for single site models based on the gauge group U(1) [8], it proved to be a good guide to such models based on SU(3) [7]. A number of studies have shown that lattice artifacts are particularly large and dangerous at nonzero μ [7] [9]. Analytic arguments for lattice QCD have been proposed which suggest that the correct behavior is recovered in the continuum [10].

Based on these considerations, we have decided to re-examine the quenched theory in greater detail, and have successfully completed a first round of simulations [11]. As will be discussed in the text which follows, our results, obtained for values of chemical potentials ranging from zero to half the pion mass, are consistent with a critical chemical potential of one third the nucleon mass, expected on physical grounds.

Unfortunately, we have not been able to adequately explore the more interesting region $\mu > m_\pi/2$ with our available resources. However,we believe that by using larger lattices and measurement techniques better tuned to the physics of nonzero chemical potential, we will be able to simulate the model successfully for chemical potentials closer to $m_N/3$.

This paper is organized into three additional sections. In Sec.II we discuss several reasons why the region of chemical potential between $m_\pi/2$ and $m_N/3$ is difficult to simulate by traditional lattice gauge theory methods which are successful at zero μ. In Sec.III we present our new 32×16^3 simulation data. These results include the first spectroscopy calculations at nonzero μ. In Sec.IV we summarize our results and give our strategies and plans for future work which, we hope, will allow us to simulate chemical potentials closer to the critical point.

II. SIMULATION PROBLEMS AT AND BEYOND $\mu = M_\pi/2$

First recall the well studied case of zero chemical potential (zero baryon number density). The normal QCD (lattice) action is quadratic in the fermion fields, so one can perform the fermion integral explicitly leading to the determinant of the Dirac operator

$$M_{n,n'} = \frac{1}{2}\sum_\lambda \eta_{n\lambda}(U_{n,\lambda}\delta_{n+\lambda,n'} - U^\dagger_{n',\lambda}\delta_{n-\lambda,n'}) + m_q\delta_{n,n'} \tag{1}$$

where n and n' label nearest neighbor sites, U are the $SU(3)$ gauge fields on the links and η the staggered quark phase factors. The new gauge action for N_f flavors is then

$$S = \sum_\square \beta(1 - \frac{1}{3}\mathrm{Tr}_\square UUUU) - \frac{N_f}{4}\mathrm{Tr}(\ln M) \tag{2}$$

which produces a partition function

$$Z = \int \mathcal{D}U e^{-S} \tag{3}$$

The expectation value of any observable f(U) is given by

$$\langle f \rangle = \frac{1}{Z}\int \mathcal{D}U f(U) e^{-S(U)} \tag{4}$$

In the quenched approximation one sets N_f to zero in the partition function. Standard Monte Carlo methods then apply to the numerical evaluation of expectation values and have been quite successful at vanishing μ.

Now we turn to the case where there is a finite chemical potential μ for quark number. This is imposed by making the replacement

$$U_{n,4} \rightarrow e^\mu U_{n,4} \tag{5}$$

and

$$U^\dagger_{n,4} \rightarrow e^{-\mu} U^\dagger_{n,4} \tag{6}$$

in the definition of M. This adds the complication that $\mathrm{Tr}(\ln M)$ is no longer real and the exponent in the definition of Z develops a phase when N_f is nonzero [2]. This problem

provides additional incentive to pursue the quenched approximation since complex actions and their attendant simulation methods, such as complex Langevin algorithms, are not well understood.

When μ is nonzero we see from the expression for the Dirac operator that quark propagation in the positive "time" direction is favored. In a diagrammatic expansion of an expectation value involving quarks there will be closed loops of quarks winding preferentially in the positive time direction. As discussed and illustrated in detail in [2], at sufficiently large μ large quark loops winding all the way around the periodic lattice in the time direction will appear. Viewing a time-slice of the partition function, this means that positive μ will favor a ground state with a net baryon density.

There are extra complications involved in inverting the Dirac operator when $\mu \neq 0$. A row in the inverse of the Dirac operator is needed in spectroscopy and chiral condensate calculations. If we use the conjugate gradient algorithm to invert M, we do this by inverting $M^\dagger M$ on the source multiplied by $M^\dagger$. This is necessary, since the conjugate gradient algorithm is designed for positive definite matrices. From the definition of M given above, it is clear that for $\mu = 0$, $M^\dagger M$ is block diagonal, connecting even sites to even sites, and odd sites to odd sites. This halves the amount of work one might naïvely have expected to perform. No such symmetry exists for $\mu \neq 0$.

For the $\mu = 0$ case the diagonal term in M is hermitean, the hopping term is skew-hermitean. Thus all eigenvalues have real part m_q. The minimum eigenvalue of $M^\dagger M$ is $\geq m_q^2$ and convergence of the conjugate gradient is guaranteed. For $\mu \neq 0$ no such simple analysis is possible. Small eigenvalues are possible and $M^\dagger M$ is relatively ill-conditioned. If no winding of the quark lines around the lattice in the time direction is possible, the matrix elements will be simply related to their $\mu = 0$ counterparts, and the fermion determinant will remain real and proportional to its $\mu = 0$ value. Once winding occurs, the system acquires a ground state with non-zero baryon number density and physics changes. Although the conjugate gradient algorithm continues to work when μ is nonzero, it converges very slowly. For example, requiring the "residual" on a 32×16^3 lattice be less than 10^{-6} then causes the

conjugate gradient routine to use approximately 650 sweeps to converge when the coupling is $\beta = 6.0$, the bare quark mass is $m_q = .02$, and the chemical potential vanishes. When μ is increased to 0.10, approximately 1,500 sweeps are needed for convergence. At $\mu = .15$ that number grows to 5,000, and at $\mu = .17$ it is typically 8,500. Many past studies of quenched QCD at nonzero μ have not faced up to the slow convergence of iterative algorithms to invert M. In fact, a number of Lanczos studies [12] simply noted that the computer time needed to find the physically relevant small eigenvalues of M grew prohibitively large at nonzero μ, and only the largest eigenvalues were obtained [13]. These partial results motivated us to study the stability and convergence of the conjugate gradient algorithm [14] as a function of the stopping residual. We are, therefore, confident that the results we present in Sec.II below are as reliable as possible.

Past studies of quenched QCD have also noted that problems begin to appear in their calculations when the chemical potential approaches $m_\pi/2$. We shall argue now that the two most important features of QCD, chiral symmetry breaking with a Goldstone pion and confinement, are responsible for these difficulties. We will see reasons why traditional lattice gauge theory calculational methods become very inefficient at nonzero μ, and we will suggest minor ways to improve them. One set of problems arises because the expected result $\mu_c = m_N/3$ relies on confinement which is a property of an ensemble average rather than a property of single configurations on which we make measurements. We will argue that there are spurious effects in the quark propagators calculated on individual gauge configurations which are large at substantial μ and yet should cancel in ensemble averages by virtue of confinement. One telltale symptom of such effects is that the approximate realization of continuum symmetries on individual configurations is no longer manifest. A second set of problems arises because the natural dispersion in $m_N/3$ and $m_\pi/2$ estimates calculated on individual configurations overlap for lattice sizes typically used at present.

To understand why one might expect algorithmic problems in calculations of hadron propagators near $\mu = m_\pi/2$ when they are calculated on individual configurations, it is simplest to consider point-to-point hadron propagators for a fixed source and sink on the

lattice. For this discussion we will consider only the exponential behavior and ignore the power-law multiplier. At $\mu = 0$ the average meson propagator has two terms at large separations T and $N_t - T$, one proportional to $exp(-m_\pi T)$, the other proportional to $exp(-m_\pi(N_t - T))$. (Here, and in what follows "proportional to" ($\propto$) is used to mean proportional to up to a T dependent phase, or in the case of the quark Green function, being a matrix in colour space, up to a T dependent matrix in colour space of unit norm (the norm of a matrix A is defined by $\sqrt{\mathrm{Tr}A^\dagger A}$.)) Empirically the pion propagator measured on individual configurations is also well approximated by 2 such terms, so we assume such an asymptotic form for the point-point meson propagator on a typical configuration. However, a meson propagator from point $x = (\mathbf{x}, 0)$ to point $y = (\mathbf{x}, T)$ on a given configuration is just $\mathrm{Tr}(G(y,x)G(x,y)) \propto \mathrm{Tr}(G^\dagger(x,y)G(x,y))$ where $G(x,y)$ is the quark propagator. This means that the quark propagator on a typical configuration must also have 2 terms, one proportional to $exp(-\frac{m_\pi}{2}T)$, the other to $exp(-\frac{m_\pi}{2}(N_t - T))$, corresponding to the quark propagating from y to x in the 2 different time directions allowed by the periodic lattice. We see immediately that this requires the meson propagator on such a configuration to have a third term, whose magnitude is less than or equal to $constant \times exp(-\frac{m_\pi}{2}N_t)$. (This constant is the geometric mean of the magnitudes of those for the first and second terms so that this statement has content.) This term is the contribution where the quark and antiquark go around the lattice in opposite directions annihilating when they meet. Since such a term is *not* allowed by confinement, contributions from different configurations must contribute with random phases and so cancel. Of course, for $\mu = 0$, this term is vanishingly small for large N_t as are terms coming from the quark winding multiple times around the lattice, so that the meson propagator remains the sum of 2 terms. The important point is that confinement is *not* a property of a single configuration (we consider the effect of translating x about the lattice as considering multiple configurations differing only by translation), but rather a result of the ensemble average.

Now let us turn to the case where $\mu \neq 0$. Here the meson propagator $\mathrm{ReTr}(G_\mu(y,x)G_\mu(x,y)) \propto \mathrm{Tr}(G^\dagger_{-\mu}(x,y)G_\mu(x,y)$, where the inclusion of the Re is the re-

sult of averaging over the given configuration and that obtained by time reversal, which is equivalent to taking $\mu \to -\mu$. For μ sufficiently small, one can use the $\mu = 0$ form for the quark propagator discussed above to argue that the quark propagator G_μ will have 2 terms, one proportional to $exp(-(\frac{m_\pi}{2} - \mu)T)$ and the other to $exp(-(\frac{m_\pi}{2} + \mu)(N_t - T))$. This means that while the first 2 terms in the meson propagator will be as before, the third term will be replaced by 2 terms the more important of which has magnitude less than or equal to $constant \times exp(-(\frac{m_\pi}{2} - \mu)N_t)$. Again, we expect such a term to cancel between configurations because of confinement. However, as μ approaches $m_\pi/2$ this term is no longer small, and for $\mu > m_\pi/2$ it, in fact, becomes large! Thus we expect the behavior of the meson propagator to change near $\mu = m_\pi/2$, varying greatly from configuration to configuration.

Now, quenched QCD has a global Z_3 symmetry which means (on the lattice) that the 3 gauge configurations differing only by having the gauge fields pointing in the +t direction from the top timeslice multiplied by a common element of Z_3, occur with the same weights in the ensemble. It is easy to see that averaging over these triplets of gauge configurations removes this third term, and all terms where the quark line winds around the lattice, except where it winds around the lattice a multiple of 3 times. The case where the quark line winds exactly 3 times around the lattice describes the configuration where the meson consists of a baryon-antibaryon pair which go round the lattice in opposite directions. Such a state is allowed, but contributes a term proportional to $exp(-(m_B - 3\mu)N_t)$. On a single configuration we would have predicted this state to behave as $exp(-3(\frac{m_\pi}{2} - \mu)N_t)$, which again becomes large near $\mu = m_\pi/2$. This ultralight 3-quark state on a typical configuration, presumably representing a state of 3 unbound quarks, must average to zero over the ensemble, as a consequence of confinement, as must the contributions of any non-colour-singlet terms leaving only the baryon contribution. Similar arguments can be applied to 6,9,... quark states.

Similar arguments indicate that $< \bar{\psi}\psi >$ for individual configurations will start acquiring extra contributions due to precocious winding of quark lines around the lattice near $\mu = m_\pi/2$, but confinement will require these to vanish in the ensemble average for $\mu < m_N/3$.

Similar effects will occur for the baryon propagator. The discussion here is more complex, since there is an additional cancellation due to confinement which occurs even at $\mu = 0$. The leading behaviour of the propagator for a 3-quark state would be expected to behave like $exp(-\frac{3m_\pi}{2}T)$ on a single configuration from our discussion above. Hence there must be cancellations of this leading behaviour which describes the propagation of 3 free quarks, if we are to get the required $exp(-m_N T)$ behaviour. Much of this cancellation occurs when we project the required colour singlet state and average the sink over the timeslice to obtain a zero momentum state. The rest of the cancellation must occur when the ensemble average binds these 3 quarks into a baryon.

Hence, even when the finite μ transition occurs at $m_N/3$ as expected, one expects to find a great increase in the statistical fluctuations of the hadron propagators near $\mu = m_\pi/2$. This is due to the fact that full confinement is not realized on a configuration by configuration basis but is rather a property of the ensemble average. Averaging over the three Z_3 boundary conditions in the t direction is expected to reduce these fluctuations by enforcing the Z_3 but not the $SU(3)$ requirements of confinement. Using, as we do, not point-point, but rather point-zero momentum (or wall-zero momentum) propagators could potentially give us some aspects of confinement. As will be discussed further in Sec.III, we explicitly average over the three Z_3 boundary conditions for each gauge configuration in an attempt to enforce the Z_3 requirements of confinement. However, our evidence is that this is insufficient to yield all aspects of confinement on a single configuration.

Another problem that can lead to considerable suppression of an estimate of μ_c found in a low statistics calculation follows from the known, large fluctuations seen in calculations of m_N. As will be discussed in Sec.III, the distributions of $m_N/3$ and $m_\pi/2$ measured on each configuration overlap even at $\mu = 0$. So, on some configurations $m_N/3$ will be as small as $m_\pi/2$ measured on the same set of configurations! In other words, the spreading in m_N will suppress estimates of μ_c to the neighborhood of $m_\pi/2$ on 32×16^3 lattices at $\beta = 6.0$. This is a conventional finite size rounding effect which should be lessened by simulating larger lattices.

For individual configurations, quark lines can wind multiple times around the lattice, even below the transition. Because the contributions of such configurations can be very large they can dominate the averages over a relatively small ensemble, giving false indications of having entered the baryon rich phase.

Such winding is the source of large fluctuations. One characteristic of such fluctuations is the fact that the hadron propagators need no longer obey the symmetries of the ensemble average (such as time reversal invariance) on a configuration by configuration basis.

Finally, let us discuss how our scenario might appear in the approach of [12] [13] which first pointed out several possible pathologies in quenched QCD. The authors used the Lanczos algorithm to determine several features of the eigenvalue distribution of M on a very small ensemble of 16^4 configurations at $\beta = 6.2$ [13]. Much of their work concentrated on Δ, the half-width of the eigenvalue distribution of M. If we are correct the outer eigenvalues of $M(m_q = 0)$ which they calculate and base their criticism on would correspond to those modes for the Dirac equation on a single configuration which cancel in observables when the ensemble average enforces confinement. Our scenario would then require that at small μ the eigenvalues of M on the imaginary axis and, in particular, near the origin have a similar distribution to that at $\mu = 0$. These eigenvalues, which are the <u>only</u> ones of direct physical significance are difficult to calculate [13] and little is know about them.

Attempts have been made to calculate the distribution of small eigenvalues of M from those of $M^\dagger M$. However, this method has potential problems. If we were indeed considering zero, and thus degenerate eigenvalues of a matrix such as M, $M^\dagger M$ could have a lower degeneracy of zero eigenvalues than M. The reason is that, if M has n zero eigenvalues, it will in general have only $m \leq n$ eigenvectors with eigenvalue zero (i.e. an *incomplete* set of eigenvectors), in which case $M^\dagger M$ has only m zero eigenvalues, not n. When this degeneracy is broken so that M has n small eigenvalues, and a complete set of eigenvectors, $M^\dagger M$ will still have only m small eigenvalues. The fact that $M^\dagger M$ might have more of its eigenvalues far from the origin than M should come as no surprise since $M^\dagger M$ admits contributions to observables where a quark-antiquark pair winding once around the lattice

together is enhanced by a factor of $exp(2\mu N_t)$. These contributions are absent for M.

New Lanczos studies of the eigenvalues of M would be very instructive, especially if they were accompanied by conjugate gradient calculation of $< \bar{\psi}\psi >$, $< J_0 >$ and spectroscopy, configuration by configuration.

III. THE SIMULATION

A. Observables

We first describe the measurements we have performed, with emphasis on the special features of the theory at finite density. They are interesting, since some give rise to relationships which hold exactly configuration by configuration, and are useful to check the convergence of the inversion. Others imply relationships which must be true only in the infinite statistics limit, and are useful to check the quality of our data sample. All of them follow from the modified symmetries of the Dirac operator:

$$M_\mu^\dagger = -M_{-\mu} \tag{7}$$

or, equivalently, from the transformation of the quark propagator G_μ under time reversal:

$$T(G_\mu(0;n)) = G_\mu(n;0) = (-1)^n G_{-\mu}^\dagger(0;n) \tag{8}$$

For the chiral condensate $< \bar{\psi}\psi >$ we then have

$$< \bar{\psi}\psi >= \mathrm{Tr}G_\mu(0;0) = \mathrm{Tr}G_{-\mu}^*(0;0) \tag{9}$$

where the second equality follows from eq. 8. Note that eq. 9 implies that $< \bar{\psi}\psi >$ is real only in the full ensemble average, when time reversal symmetry must be realized.

In our particular simulation, we used a noisy estimator for $< \bar{\psi}\psi >$. So, in our case eq. 9 must hold only when the average over the noise is taken. We thus lose this convergence test on isolated configurations, but we can check a posteriori the statistical quality of our sample by verifying (9) for the ensemble.

Similar remarks hold for the charge operator $< J_0 >$, obtained by differentiating the action with respect to the chemical potential. As discussed in [2] $< J_0 >$ is the expectation value of the number of paths in the t direction.

In addition to independent calculations for positive and negative chemical potential for each configuration, we calculated all observables for the three different Z_3 (antiperiodic) boundary conditions defined by

$$\psi(t + N_t) = (-1)e^{i(2\pi k/3)}\psi(t); \quad k = (0, 1, 2) \tag{10}$$

to enforce some of the constraints of confinement configuration by configuration.

The spectrum computation is more delicate: in the meson sector we have to compute

$$C^i_{q\bar{q}}(T) = \sum TrG_\mu(0;n)\Gamma_i G_\mu(n;0)(-1)^n \tag{11}$$

where Γ_i stands for the generic combination of gamma matrices associated with each meson. Inserting (8) we see that $C^i(t)$ should be computed according to

$$C^i_{q\bar{q}}(T) = \sum TrG_\mu(0;n)\Gamma_i G^\dagger_{-\mu}(0;n) \tag{12}$$

(unless we want to compute the fermion propagator with a source at all points of the lattice), and this requires the inversion of the Dirac operator with opposite values of the chemical potential, representing the contributions of quark and antiquark, respectively.

The same property (8) together with shift invariance in t gives the following symmetry for the propagators C_i which must hold for ensemble averages:

$$C^i_{q\bar{q}}(T) = C^i_{q\bar{q}}(N_t - T) \tag{13}$$

In the ensemble average we thus recover (at least in the confined phase, where both of the above mentioned symmetries hold) the usual parametrization for the meson propagators. The standard sum rule (Ward identity) holds configuration by configuration in the modified form

$$< \bar{\psi}\psi >_\mu = m_q \sum_T C^\pi_{q\bar{q}}(T) \tag{14}$$

$$< \bar{\psi}\psi >_{-\mu} = m_q \sum_T C^{\pi}_{\bar{q}q}(T) \tag{15}$$

which gives again eq. 9

$$< \bar{\psi}\psi >_{\mu} = < \bar{\psi}\psi >^{*}_{-\mu} \tag{16}$$

For the nucleon things are different: the only exact relationship in the ensemble average is:

$$C^{N}_{qqq}(t) = (-1)^T C^{N}_{\bar{q}\bar{q}\bar{q}}(N_t - T) \tag{17}$$

and no simple relationships exist between $C_{qqq}(T)$ and $C_{qqq}(N_t - T)$. In other words for the baryon the usual parametrization is modified due to the different behaviour in backward and forward propagation induced by finite μ: the "minimal" baryon propagator at finite density contains at least two positive parity excitations. It is clear that finite size effects are, also from this point of view, especially severe.

In all our spectrum measurements we made use of a wall source [15], after the appropriate gauge fixing. In this way our propagators reach their asymptotic regime faster, but we pay the price of an amplification of the non-positivity effects connected with finite density.

Also, for the spectrum computation we calculated all observables for the three different Z_3 (antiperiodic) boundary conditions defined in eq. 10. Since masses are non-linear observables, we may expect that the results obtained by averaging the masses obtained on subsamples corresponding to fixed boundary condition are different from those obtained after averaging the propagators on all the three boundaries, for our *finite* ensemble. Such behaviour, if present, would provide evidence of winding loops, which have yet to cancel.

B. Numerical analysis

The theory at finite density was simulated on a $16^3 \times 32$ lattice, at bare quark mass $m_q = .02$ and $\beta = 6.0$. For these parameters, the mass of the baryon at zero density is .77 and the mass of the pion is .34. The region of the chemical potential we have successfully

explored ranges from zero to $m_\pi/2 = .17$. We have also made some exploratory runs at $\mu = .2$.

The results we discuss below result from 30 configurations with the first boundary condition, 19 with the second , and 19 with the third analyzed at $\mu = .0$, (30+19+19)$\times$ 2 at $\mu = .1$, (30+30+30) $\times$ 2 at $\mu = .15$, and (44+44+44)$\times$ 2 at $\mu = .17$, (26+26+26)$\times$2 at $\mu = .2$ (recall that at $\mu \neq 0$. we solve the Dirac equation for positive and negative μ).

Our configurations were generated by an admixture of Metropolis and overrelaxed algorithms. We analyzed them every 10000 sweeps, after initially discarding 12000 sweeps for thermalization.

We begin by discussing the behaviour of the chiral condensate and number density. A few comments are in order. First, the fluctuations increase strongly with μ. Second, the different boundaries give rise to slightly different results even at $\mu = 0$. Finally by increasing μ we observe several configurations in which the results obtained with opposite μ values are completely different. Clearly, a finite chemical potential amplifies the inhomogeneities of the single configurations (note that such differences would vanish were we to average over our noisy sources).

We have verified that the results for the chiral condensate and number density obtained with $\pm\mu$, and with the three different boundaries, are mutually consistent. We thus average over them configuration by configuration, and we show in Figs. 1 and 2 the resulting histograms. Their main characteristic (which is common to all the μ values) is the absence of a two peak signal, which would suggest a phase transition. The results change smoothly from $\mu = 0$ to $\mu = .17$, while at $\mu = .2$ the results are much noisier. The regular structure of the distributions gives us confidence that in the entire range of μ studied here the system is in the chirally broken phase (note, however, that most of the chiral condensate comes from the explicit symmetry breaking mass term : at zero μ, $< \bar{\psi}\psi >= .13$ and only .03 is due to spontaneous symmetry breaking [16]). From Figs. 1 and 2 we can also appreciate the increasing width of the distributions with μ, and the presence of scattered events. As a further consistency check, we also performed partial analyses discarding those values which

deviated most strongly from the average. Nonetheless, we consistently found compatible results. So, the situation is well under control from the statistical point of view, and our data for the chiral condensate and number density do not show any sign of a phase transition.

The spectroscopic analysis posed more specific problems. As stated above, we are dealing with non-positive definite operators. Violation of positivity is also possible because of the wall source we are using. These effects are so significant that they even produced a few pion propagators which are negative at zero distance! Another dramatic feature in some of our propagators are huge fluctuations: when that occurs, the shape of the propagator is altered as well. This contrasts with the situation at zero chemical potential, where amplitudes may be fluctuating, even strongly, but the hyperbolic cosine behaviour is preserved, even, for instance, in the 'exceptional' configurations observed with Wilson fermions near κ_c. To be more specific, we show in Fig. 3 a(b) the collection of the pion (baryon) propagators at $\mu = .15$, where the problem was observed first (note that the exceptional propagator even has the 'wrong' symmetry!). In Fig. 4a(b) we show the same data at $\mu = .17$. The change in behaviour while increasing μ is dramatic: however, the expected hyperbolic cosine pattern is still visible, and the average propagators do not show qualitative pathologies.

What is the origin of these exceptional configurations? What will ultimately occur in the limit of large statistics? The most natural explanation is the occurrence of zero modes, and the question to be answered concerns their physical significance. As discussed in Sec.II, isolated zero modes in quark propagators calculated on individual configurations can still be compatible with confinement and chiral symmetry breaking.

Here we want to suggest that (1.) the origin of these exceptional configurations may be completely trivial, simply related to statistical fluctuations, as anticipated in the Introduction; and, (2.) to provide arguments which support their suppression in the continuum, infinite volume limit.

To make our point clear, it is useful to characterize the behaviour of a configuration by the effective masses, both for the pion and baryon. For the effective mass analysis we have extracted the direct channel according to [17]

$$G_{direct}(2t) = 2G(2t) + G(2t+1) + G(2t-1) \tag{18}$$

(We have systematically checked that the results of global fits give compatible, although less accurate, results.) Also, for the baryon we took into account the modified parametrization discussed above simply by analyzing half of the lattice, which is justified by the fast decay of the baryon correlators.

To begin, we show in Fig.5 the results from the effective mass analysis at $\mu = 0$ for half the pion mass and for one third the baryon mass performed on individual configurations. From Fig.5 we can see an overlap between half the pion mass, and one third of the baryon mass, which is better demonstrated by the relative histogram, Fig. 6.

Let us now consider the behaviour at $\mu = .17$, first for the pion mass (we are using now only those propagators which give positive numbers for the effective masses). In Fig. 7 we compare the distribution of (half the) pion mass at these two μ values: the distribution spreads out while increasing μ, an effect already observed in the measurements of the chiral condensate and the number density. Of course on the left the distribution is bounded by zero, which results in an asymmetric shape.

Analogously, we show in Fig.8 the results for the baryon: in this case, in addition to the spreading, we observe also a shift in its central value. (We will see later on that the shift in one third of the baryon screening mass is μ. Here we also plot the distribution shifted by μ which, modulo the spreading, coincides with the one at $\mu = 0$.) Again, the left wing of the distribution is "missing".

In both cases (pion and baryon) we may associate the pathological configurations with the ones which should populate the left part of the distribution. The following scenario is certainly possible: the pion mass distribution has half-width $\Delta = \Delta(m_q, L, \mu, \beta)$. The pion mass (i.e. the central value of the distribution) does not change in the confined phase. However, the first zero modes show up when $m_\pi - \Delta(m_q, L, \mu, \beta) = 0$, around half the mass of the pion in this simulation. Since $\lim_{L\to\infty,\beta\to\infty} \Delta = 0$ this pathology is a lattice artifact, and the quenched theory should make perfect sense in the continuum, infinite volume limit.

An analogous argument can be made for the baryon.

This mechanism, which is simply derived from the natural fluctuations at finite size and spacing, is enough to account for the apparent early onset of the chiral transition reported in the past. We cannot of course exclude that other more fundamental pathologies affect the theory at finite density. Only simulations on larger lattices, and possibly closer to the continuum, can definitively settle the issue.

We now turn to the conventional effective mass analysis. Again, the results obtained for the three different boundary conditions were fully consistent. We averaged over them. At $\mu = .15$ and .17 we had to eliminate the exceptional configurations (only one, actually, at $\mu = .15$) in order to obtain rather clean results for the effective masses. We stress however that the results of global fits performed on the full sample, although very noisy, are compatible with those obtained by the effective mass analysis on a selected subsample. The results for the effective masses are shown in Fig. 9 for the pion, and 10 for the baryon.

C. Results.

In table I we report the results for the chiral condensate and the number density. The data was averaged over the three different boundaries, and over $\pm\mu$. We quote also the imaginary parts, which are consistent with zero, as they should be. Fig. 11 shows the corresponding plots.

Table II shows the results for the pion and baryon masses. As discussed above, at this stage in our ongoing project, we quote our results for the effective mass analysis at $\mu = .15$ and .17, with the caveat that they have been obtained on a subsample. We can justify this procedure in part by noting that the results from the fits on the full sample are fully consistent, with enlarged statistical errors, with the ones we quote. The screening masses are plotted as a function of μ in Fig. 12.

The results can be summarized as following:

$$J_0(\mu) = J_0(0)$$

$$< \bar{\psi}\psi > (\mu) = < \bar{\psi}\psi > (0)$$

$$m_\pi(\mu) = m_\pi(0)$$

$$m_N(\mu) = m_N(0) - 3\mu \tag{19}$$

This trend, if maintained, would give $\mu_c = m_N/3$.

Again, recall that the term 3μ in the baryon screening mass is expected of simple quark models of nuclear matter. They predict that the nucleon screening mass will decrease linearly with increasing chemical potential μ and a chiral symmetry restoration transition will occur at $\mu = m_N/3$.

IV. DISCUSSION AND PROSPECTS FOR FUTURE WORK

In summary, we believe that the criticism and pathologies of quenched QCD pointed out in the past can be interpreted in terms of the fluctuations expected for $\mu \gtrsim m_\pi/2$ as discussed in Sec. 2 above. It need not be true that quenched QCD is unreliable at nonzero μ. We believe, in fact, that the difficulties in simulating quenched QCD at nonzero μ will be equally severe in the full theory, but both classes of simulations will be ultimately successful. The constraints of confinement are, we believe, absolutely essential to obtain physical results from simulations at nonzero chemical potential and, as we have argued above, the traditional simulation scheme for lattice QCD is not well suited for this purpose.

We are now preparing a new set of simulations. Our past measurements made use of a wall source for spectroscopy, and of a noisy estimator for $\langle\bar{\psi}\psi\rangle$. We are now testing a "noisy" wall source. Such a source is obtained from our simple wall source by performing a random gauge transformation. This source gives us a stochastic estimator of the hadron propagators for a point source, averaged over all points on the source time-slice. A point source gives, in general, propagators which are more poorly behaved than those produced by a wall source. However, averaging over a large enough ensemble, a noisy source has the advantage of also averaging over all points on the source time-slice, increasing our effective ensemble size by a factor equal to the number of *independent* point sources on the time-slice. This approach

should increase the effective ensemble size and reduce the variance by enforcing confinement. We believe such an effect is the reason why our stochastic estimator for $\langle\bar{\psi}\psi\rangle$ is much better behaved when we enter the region $\mu \gtrsim m_\pi/2$ than the hadron propagators obtained from a simple wall source [15].

We are also planning a simulation on a larger, 64×16^3, lattice. Larger lattices should help control all the possible pathologies discussed in Sec.II : the constraints of confinement are clearer on larger lattices, variances in effective masses are diminished and violations of symmetries are suppressed. Since we will also be using the better measurement techniques discussed above, we are hopeful that we will obtain more decisive simulation results for μ between $m_\pi/2$ and $m_N/3$. In addition, the increase of N_t further decreases the temperature $(1/N_t)$ of the lattice, which also helps suppress pathologies.

We would like to thank Ian Barbour and Eduardo Mendel for interesting conversations.

This work was supported in part by NSF via grant NSF-PHY92-00148 and by DOE contract W-31-109-ENG-38. Simulations were done using the CRAY C-90 at NERSC.

DISCLAIMER

This report was prepared as an account of work sponsored by an agency of the United States Government. Neither the United States Government nor any agency thereof, nor any of their employees, makes any warranty, express or implied, or assumes any legal liability or responsibility for the accuracy, completeness, or usefulness of any information, apparatus, product, or process disclosed, or represents that its use would not infringe privately owned rights. Reference herein to any specific commercial product, process, or service by trade name, trademark, manufacturer, or otherwise does not necessarily constitute or imply its endorsement, recommendation, or favoring by the United States Government or any agency thereof. The views and opinions of authors expressed herein do not necessarily state or reflect those of the United States Government or any agency thereof.

REFERENCES

[1] See, for instance, the contributions of B. Muller and J. W. Harris to the Proceedings of the NATO Advanced Study Institute on Particle Production in Highly Excited Matter, Plenum (1993)

[2] J. B. Kogut,H. Matsuoka, M. Stone,H. W. Wyld, S. Shenker, J. Shigemitsu and D. K. Sinclair , Nucl.Phys. **B225** [FS9], 93 (1983).

[3] P. Hasenfratz and F. Karsch, Phys.Lett.**125B**, 308 (1983).

[4] A recent review is I. Barbour, Nucl. Phys. **B** (Proc. Suppl.) 26,22 (1992).

[5] F. Karsch and H. W. Wyld, Phys. Rev. Lett. **55**, 2242 (1985); N. Bilić, H. Gausterer and S. Sanielevici, Phys. Rev. **D37**, 3684 (1988).

[6] E. Mendel, Nucl. Phys. **B387**, 485 (1992).

[7] N.Bilić and K. Demeterfi, Phys. Lett. **B212**, 83 (1988).

[8] P.E. Gibbs, Phys. Lett. **B182**, 369 (1986).

[9] J. Vink, Nucl.Phys.**B323**, 399 (1989).

[10] N.Bilić, K. Demeterfi and B.Petersson, Nucl.Phys. **B377**, 651 (1992).

[11] J. B. Kogut, M.-P. Lombardo and D. K. Sinclair, contribution to the Proceedings of the Lattice93 Conference, Dallas, October 12–16 1993, to be published.

[12] I. Barbour, N-E Behilil, E. Dagotto,F .Karsch, A. Moreo,M. Stone and H. W. Wyld, Nucl.Phys.**B275** [FS17], 296 (1986).

[13] C. T. H. Davies and E. G. Klepfish, Phys. Lett. **B256**, 68 (1991), and references therein.

[14] L. A. Hageman and D. M. Young, Applied Iterative Methods, Academic Press, London (1981); M. R. Hestenes and E. L. Stiefel, Nat. Bur. Std. J. Res. **49**, 409 (1952).

[15] For a description of wall sources measurements, see for instance R. Gupta et al., Phys. Rev **D43**, 2003 (1991), and references therein.

[16] Communicated by S. Kim.

[17] J. P. Gilchrist et al., Nucl. Phys. **B248**, 29 (1984).

TABLES

μ	Re $< \bar{\psi}\psi >$	Im $< \bar{\psi}\psi >$
0.000	0.13769 (60)	-0.0006(10)
0.100	0.13750 (70)	-0.0021(11)
0.150	0.1362 (18)	-0.0001(13)
0.170	0.1359 (19)	-0.0051(21)
0.200	0.121 (4)	-0.0027(65)
μ	Re $< J_0 >$	Im $< J_0 >$
0.000	-0.00047(98)	-0.00085(64)
0.100	0.00033(83)	-0.00010(76)
0.150	0.00069(145)	-0.0022(12)
0.170	0.00071(162)	0.0007(17)
0.200	0.004(5)	0.0009(7)

TABLE I. Results for the chiral condensate and the number density as a function of μ

μ	m_π	m_N
0.000	0.3396(36)	0.741(15)
0.100	0.3374(75)	0.442(14)
0.150	0.3182(52)	0.292(22)
0.170	0.313(15)	0.235(24)

TABLE II. Results for the pion and the baryon screening mass as a function of μ

FIGURES

FIG. 1. Frequency plot for the chiral condensate at $\mu = 0$ (a) and $\mu = .17$ (b). For each configuration we averaged over the three boundaries, and the opposite μ values.

FIG. 2. Frequency plot for the number density $< J_0 >$ at $\mu = 0(a)$ and $\mu = .17$ (b). For each configuration we averaged over the three boundaries, and the opposite μ values.

FIG. 3. Pion(a) and baryon(b) propagators obtained with the first boundary condition at $\mu = .15$

FIG. 4. Same as Fig. 3 for $\mu = .17$

FIG. 5. Effective masses computed configuration by configuration for the $m_\pi/2$ (circles) and $m_B/3$ (squares) at $\mu = 0$.

FIG. 6. Histograms accompanying Fig. 5. Dash is for $m_\pi/2$ and solid is for $m_N/3$.

FIG. 7. Histograms for $m_\pi/2$ at $\mu = .17$ (solid). The histogram at $\mu = 0$ is shown for comparison (dash).

FIG. 8. Histograms for $m_N/3$ at $\mu = .17$ (solid). The same, shifted by μ (dot). The histogram at $\mu = 0$ is shown for comparison (dash).

FIG. 9. Effective masses for the pion as a function of time, for $\mu = (0, 0.1, 0.15, 0.17)$, (crosses, diamonds, squares, circles).

FIG. 10. Effective masses for the nucleon as a function of time, for $\mu = (0, 0.1, 0.15, 0.17)$, (crosses, diamonds, squares, circles).

FIG. 11. $< J_0 >$ (a) and $< \bar{\psi}\psi >$ (b) as a function of μ.

FIG. 12. Pion (crosses) and baryon (circle) masses as a function of μ. The straight line is $y = m_B(0) - 3\mu$.

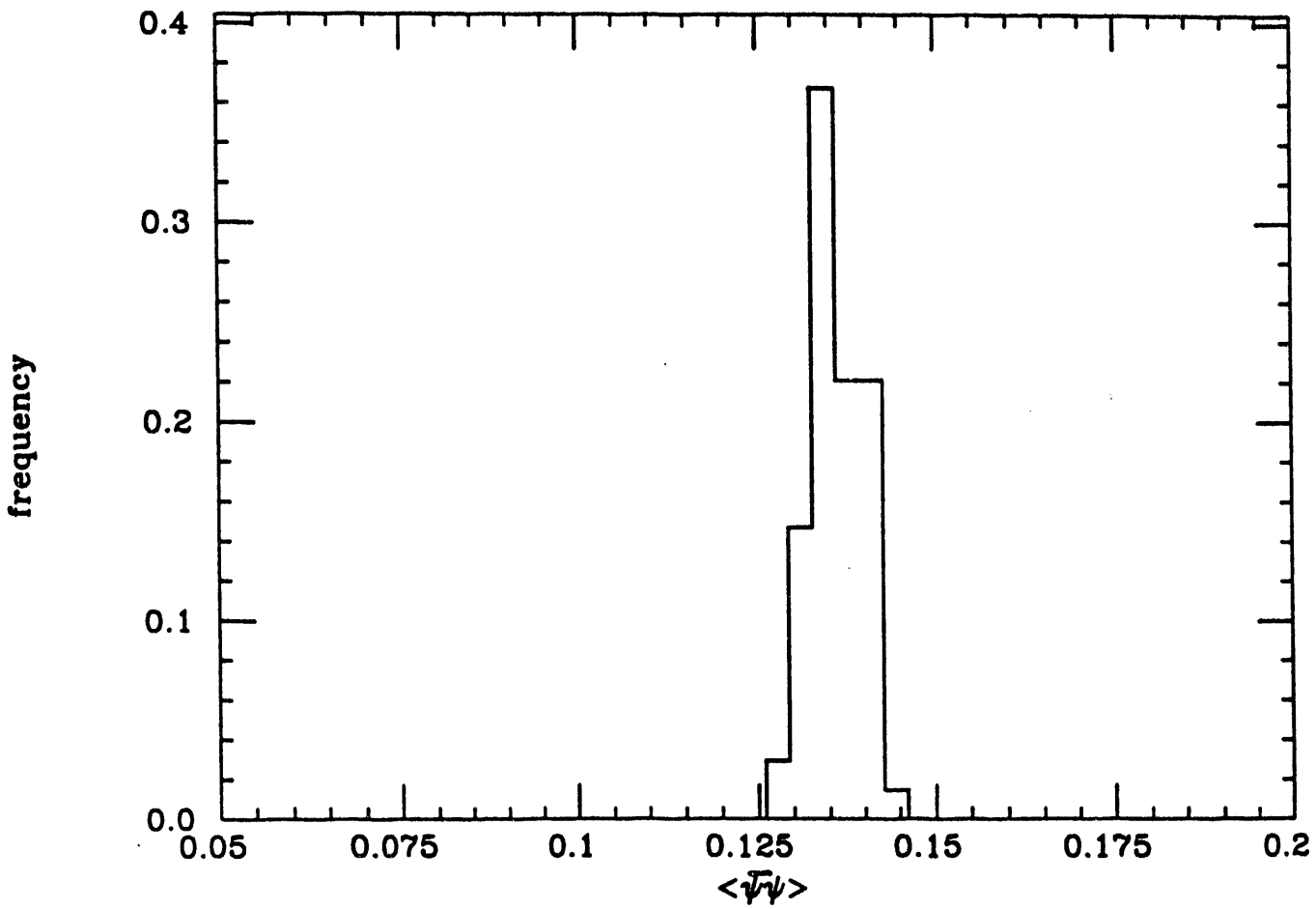

Fig. 1a

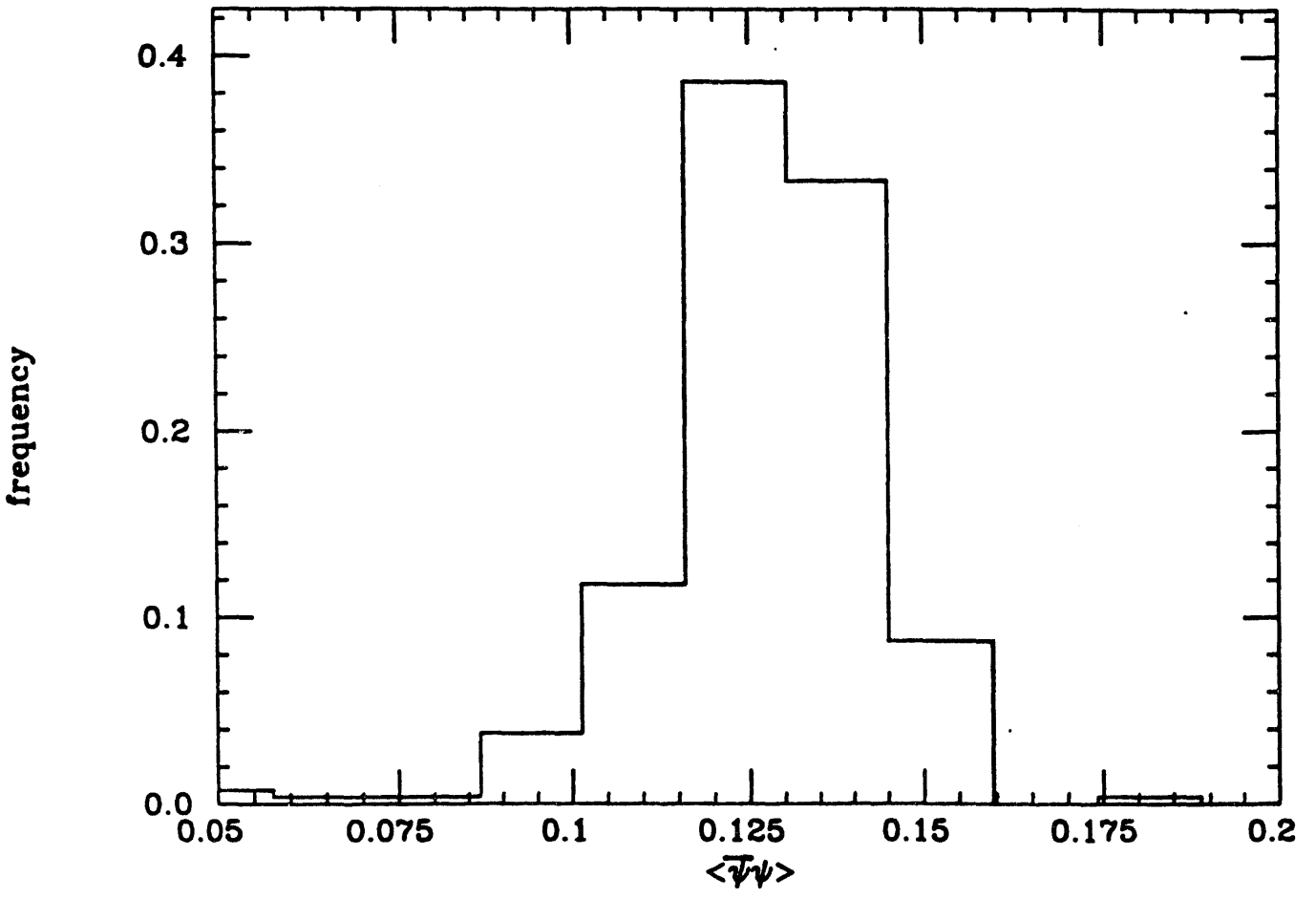

Fig. 1b

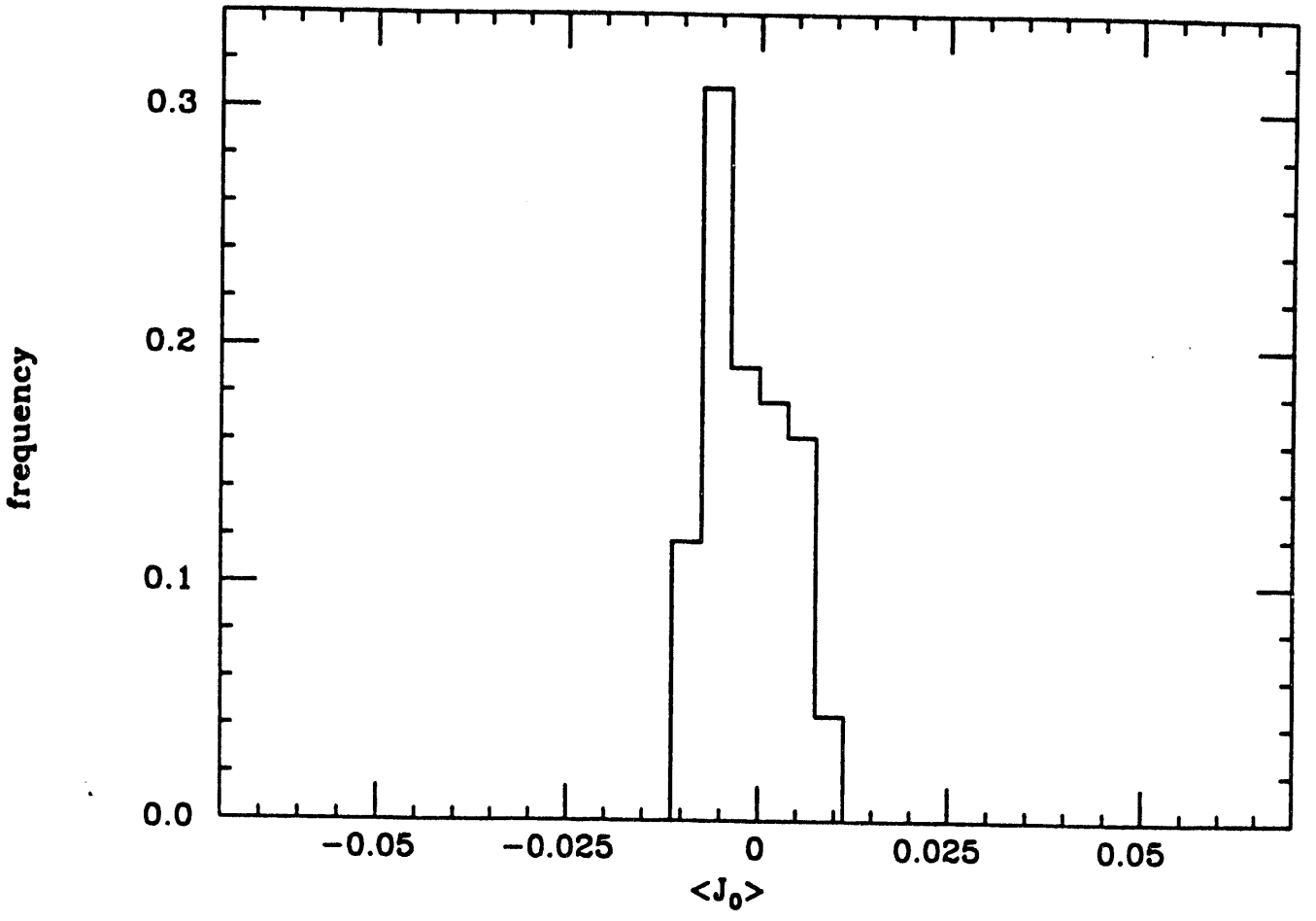

Fig. 2a

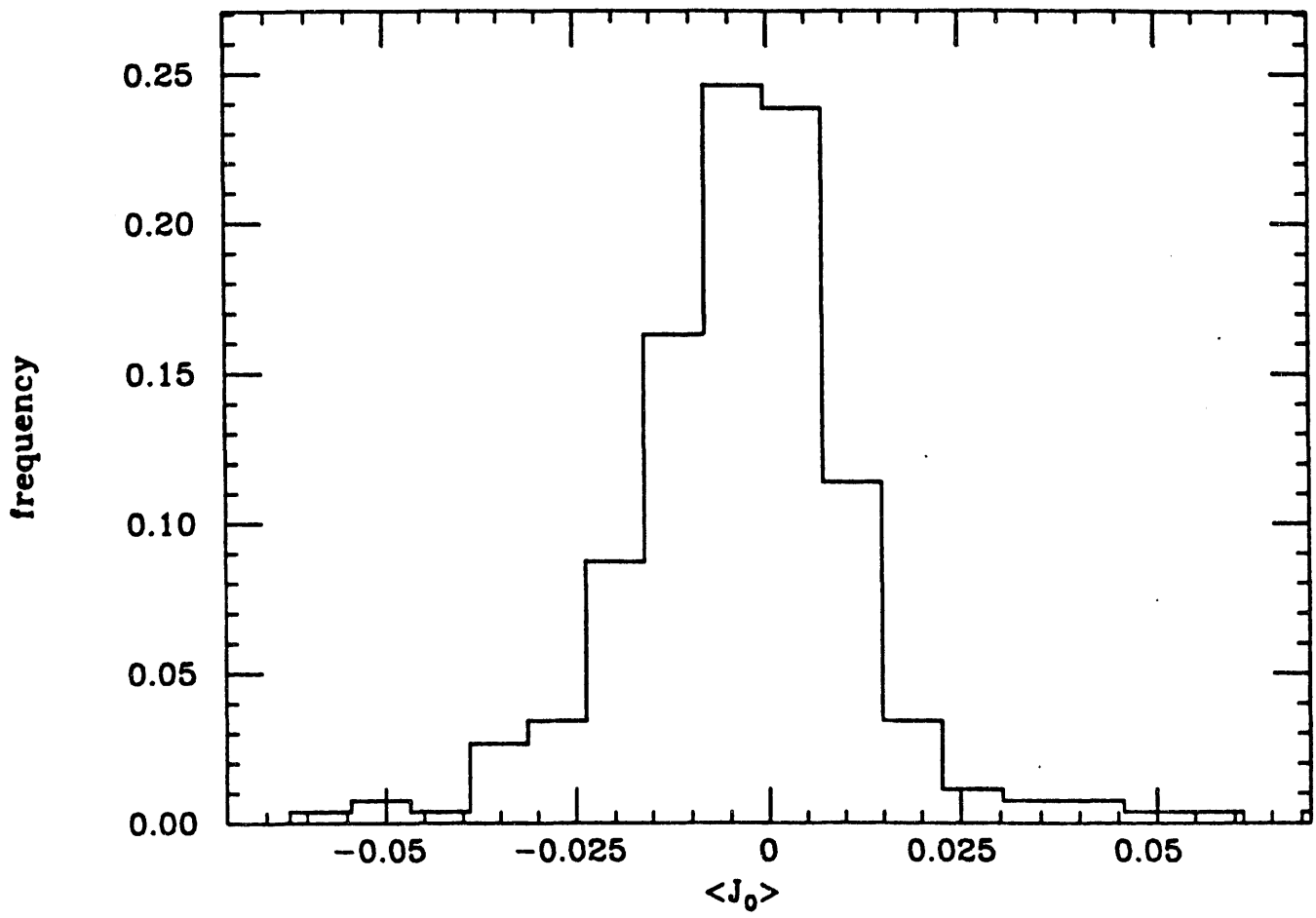

Fig. 2b

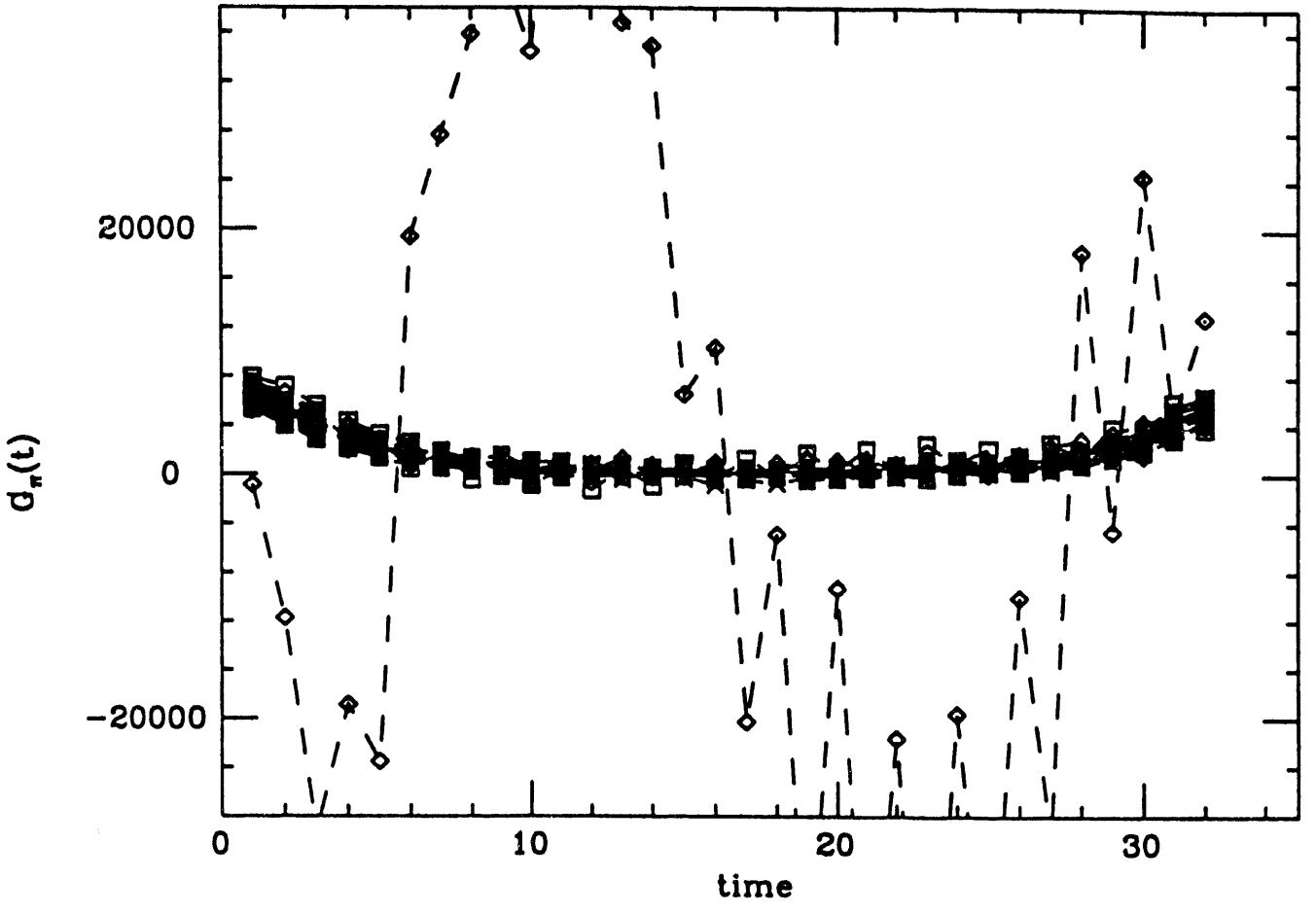

Fig. 3a

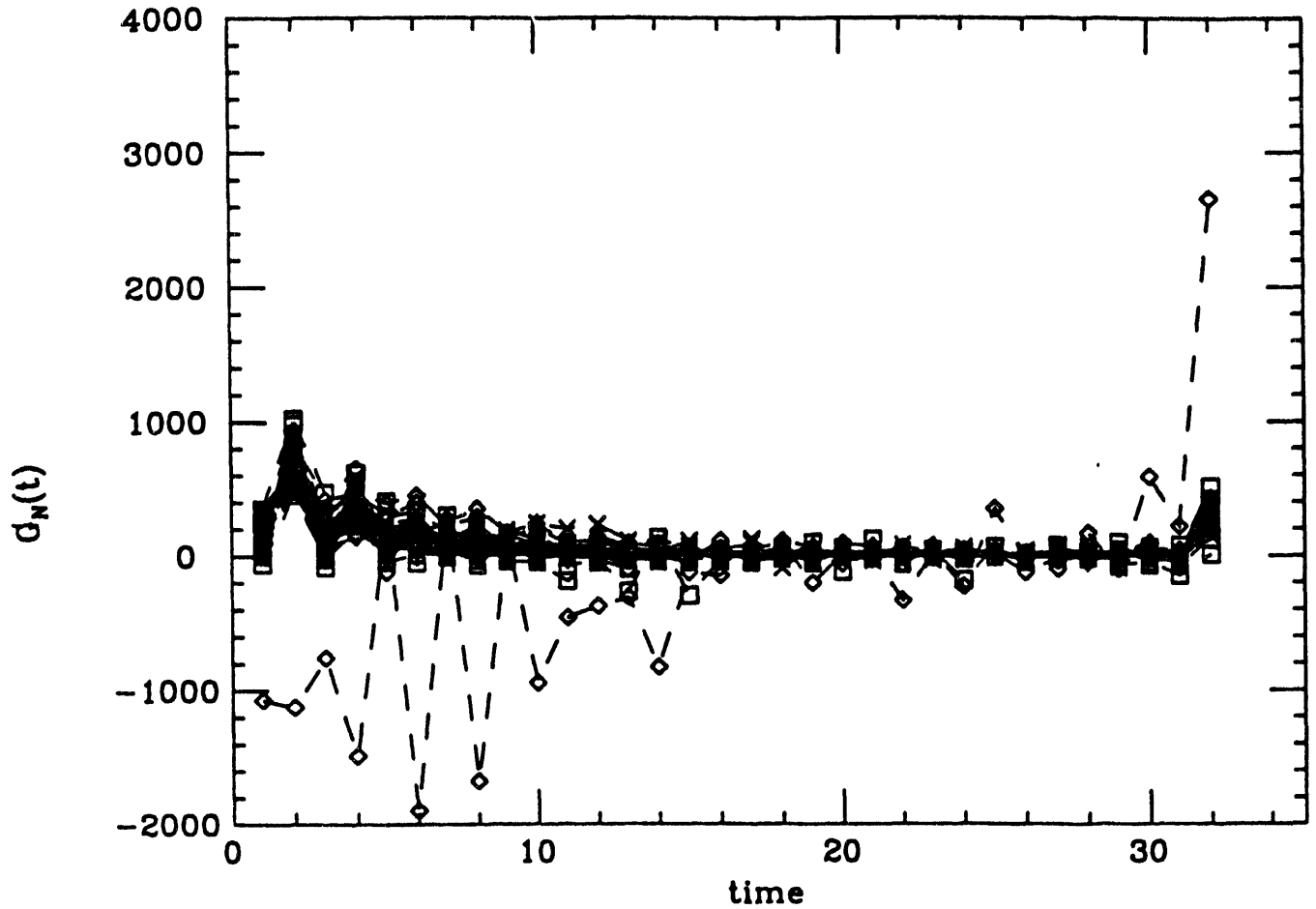

Fig. 3b

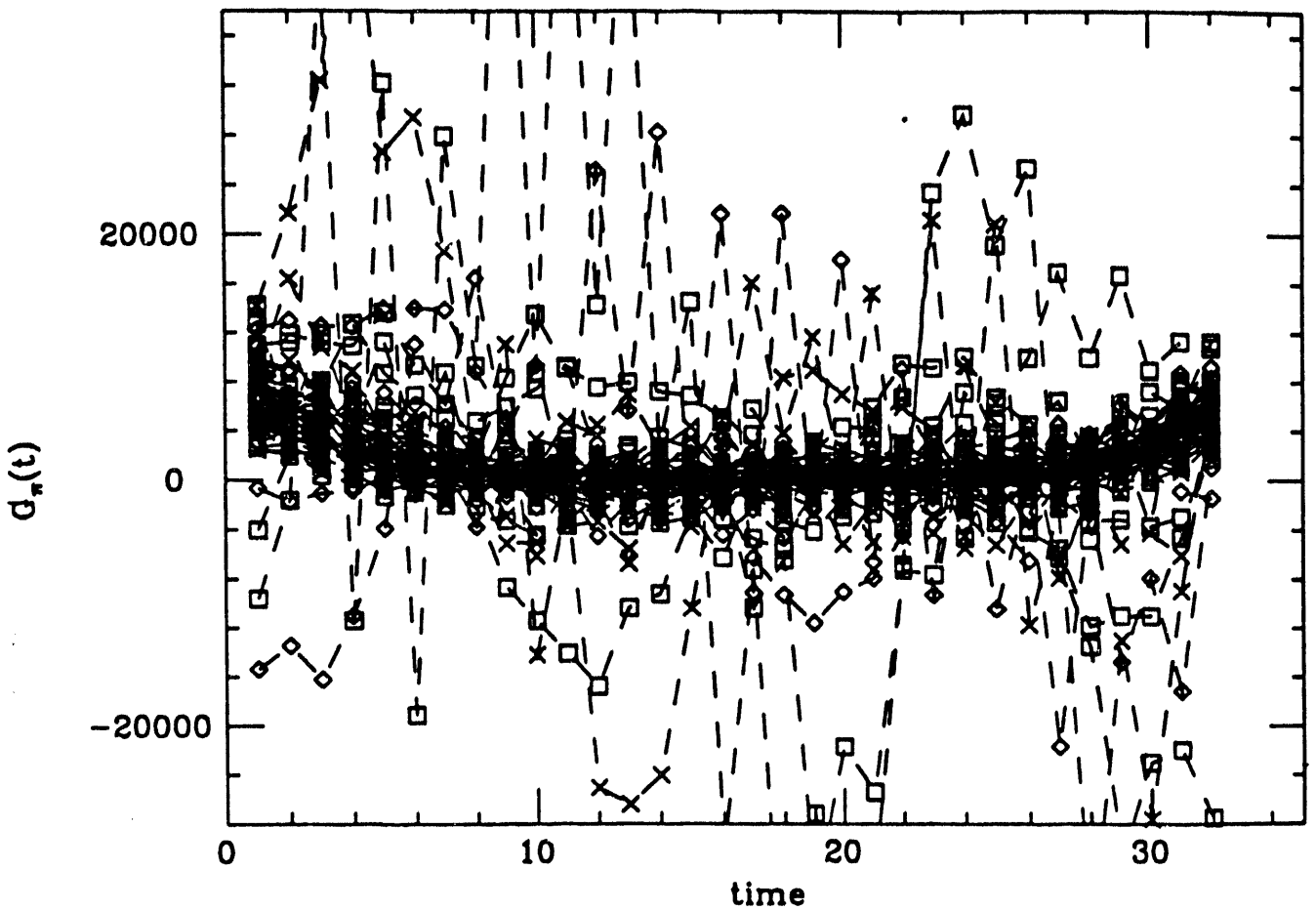

Fig. 4a

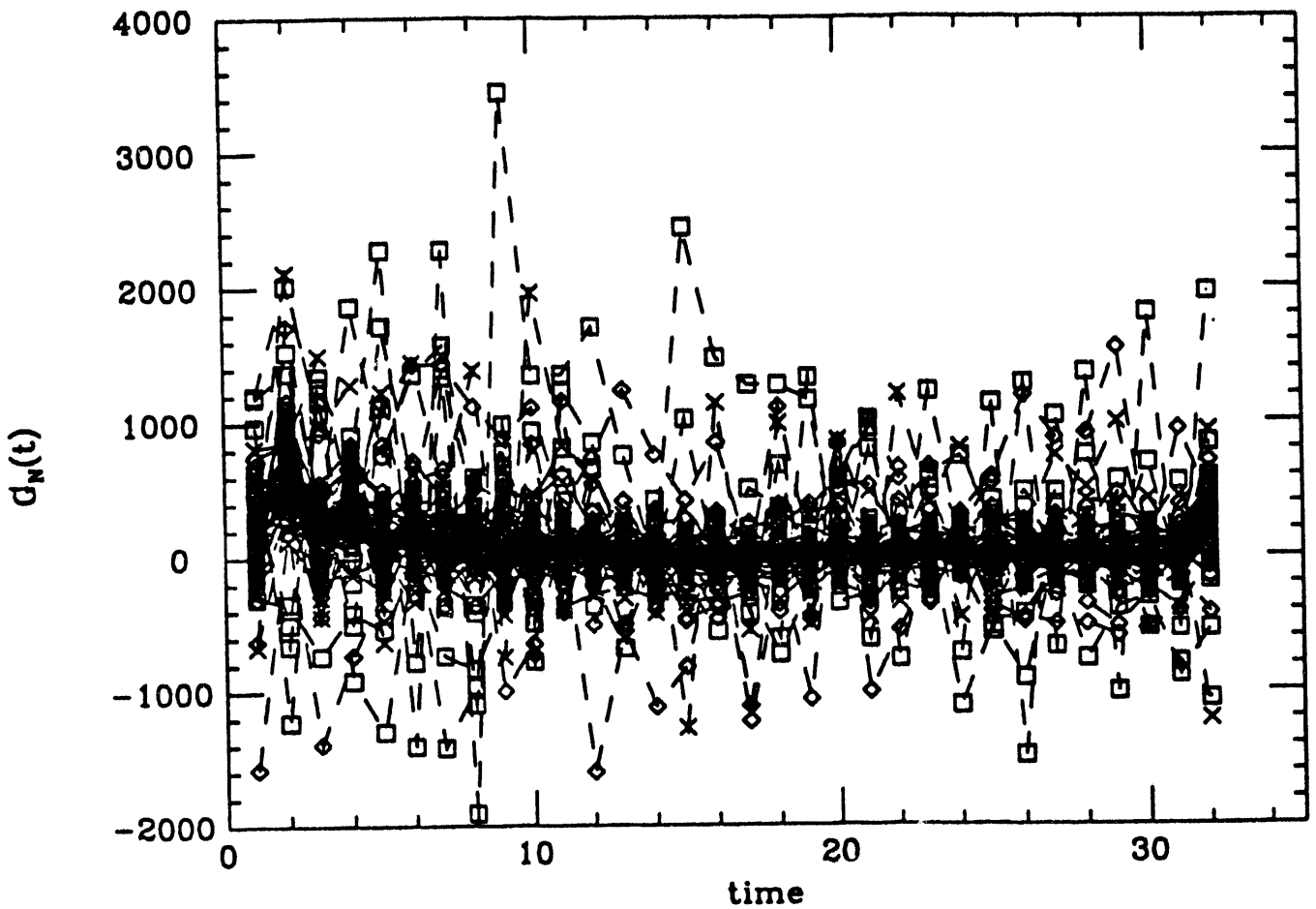

Fig. 4b

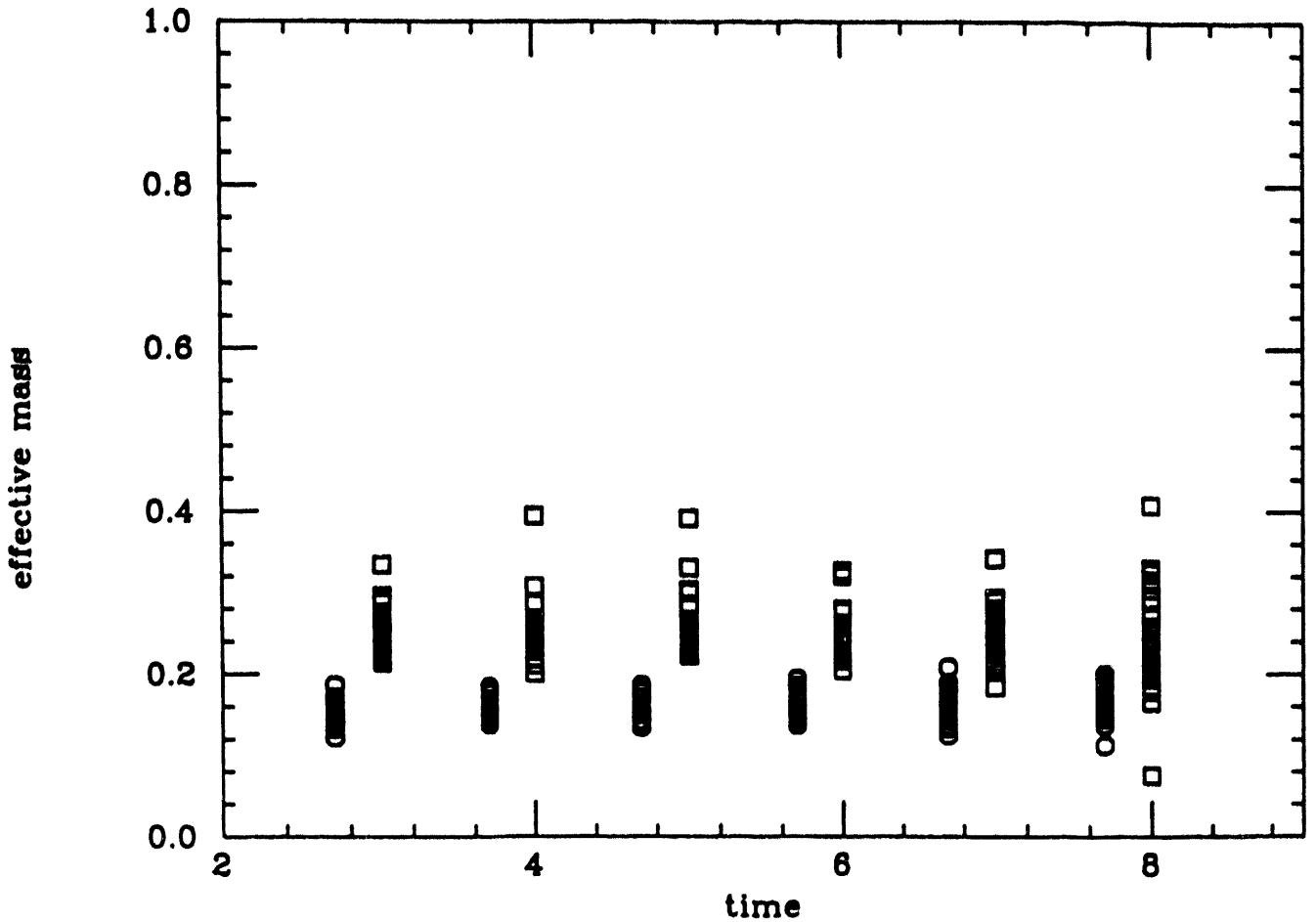

Fig. 5

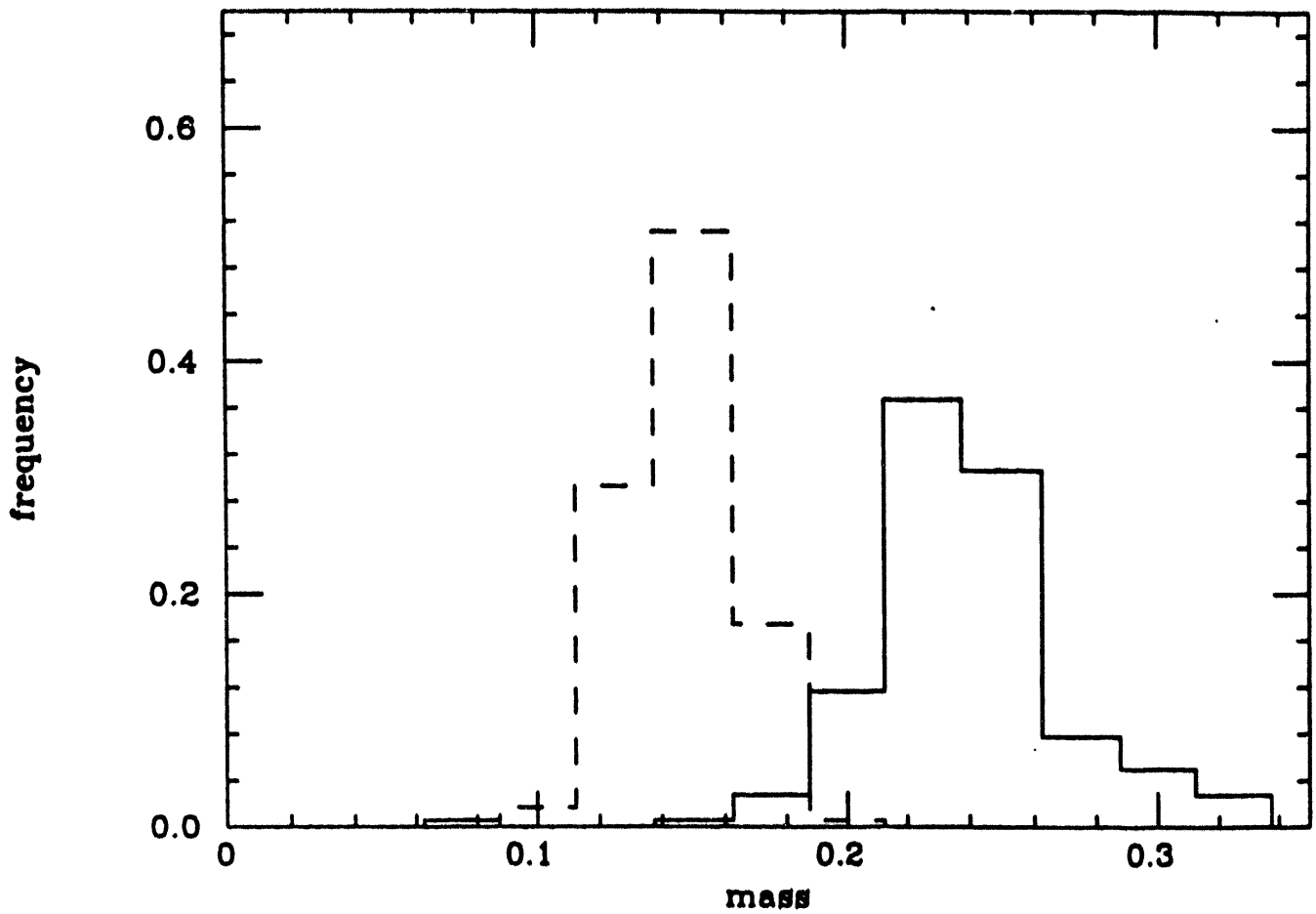

Fig. 6

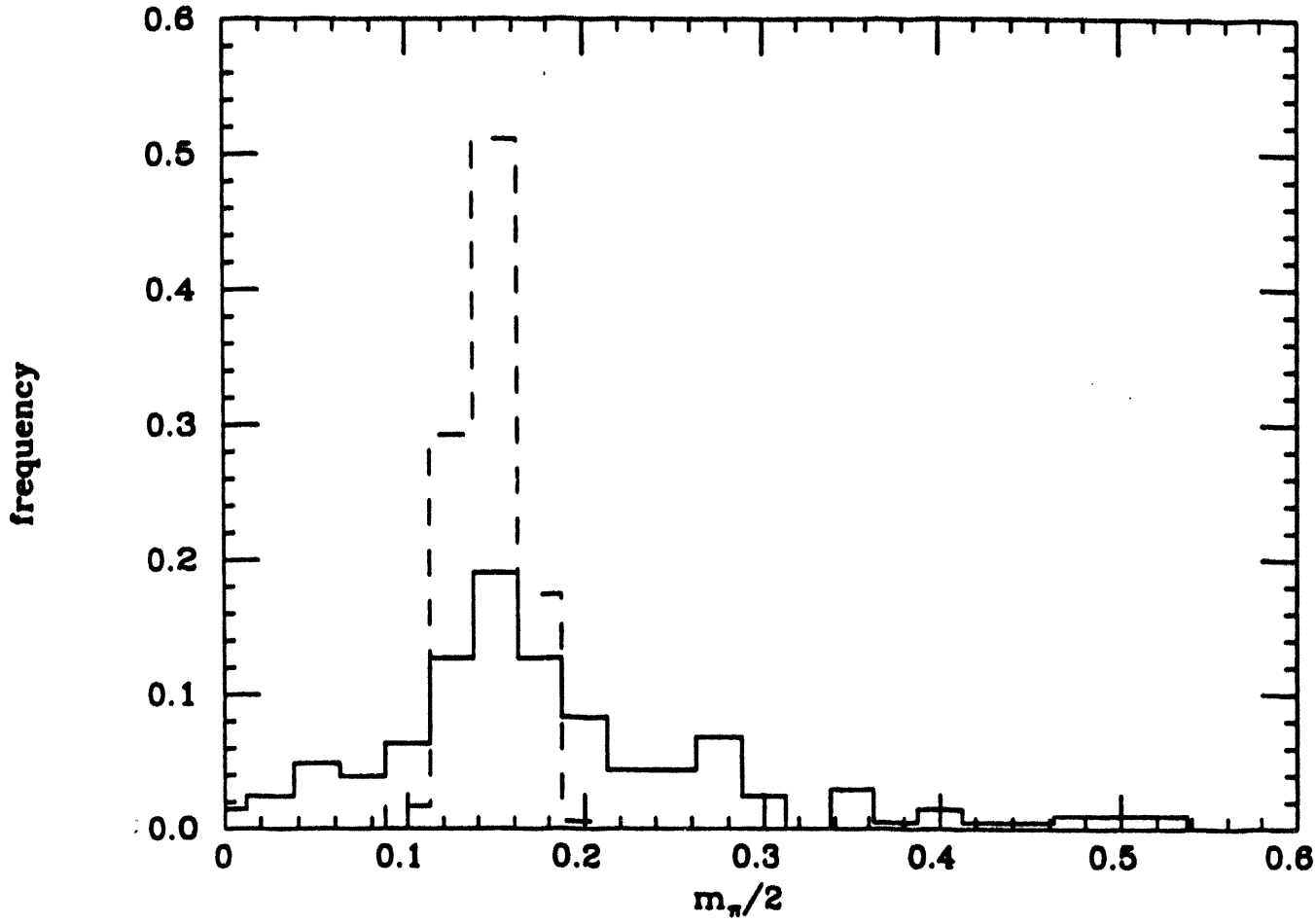

Fig. 7

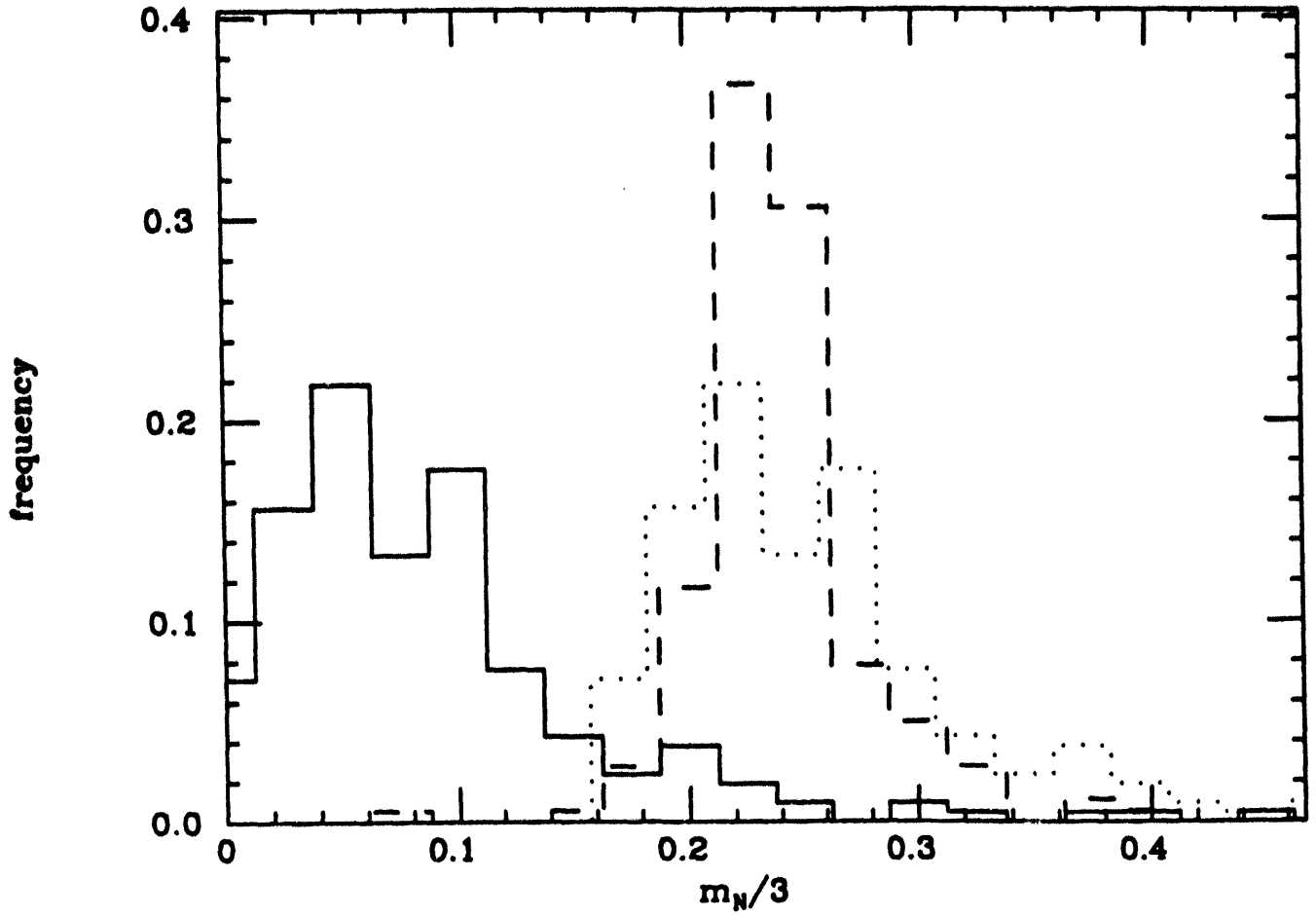

Fig. 8

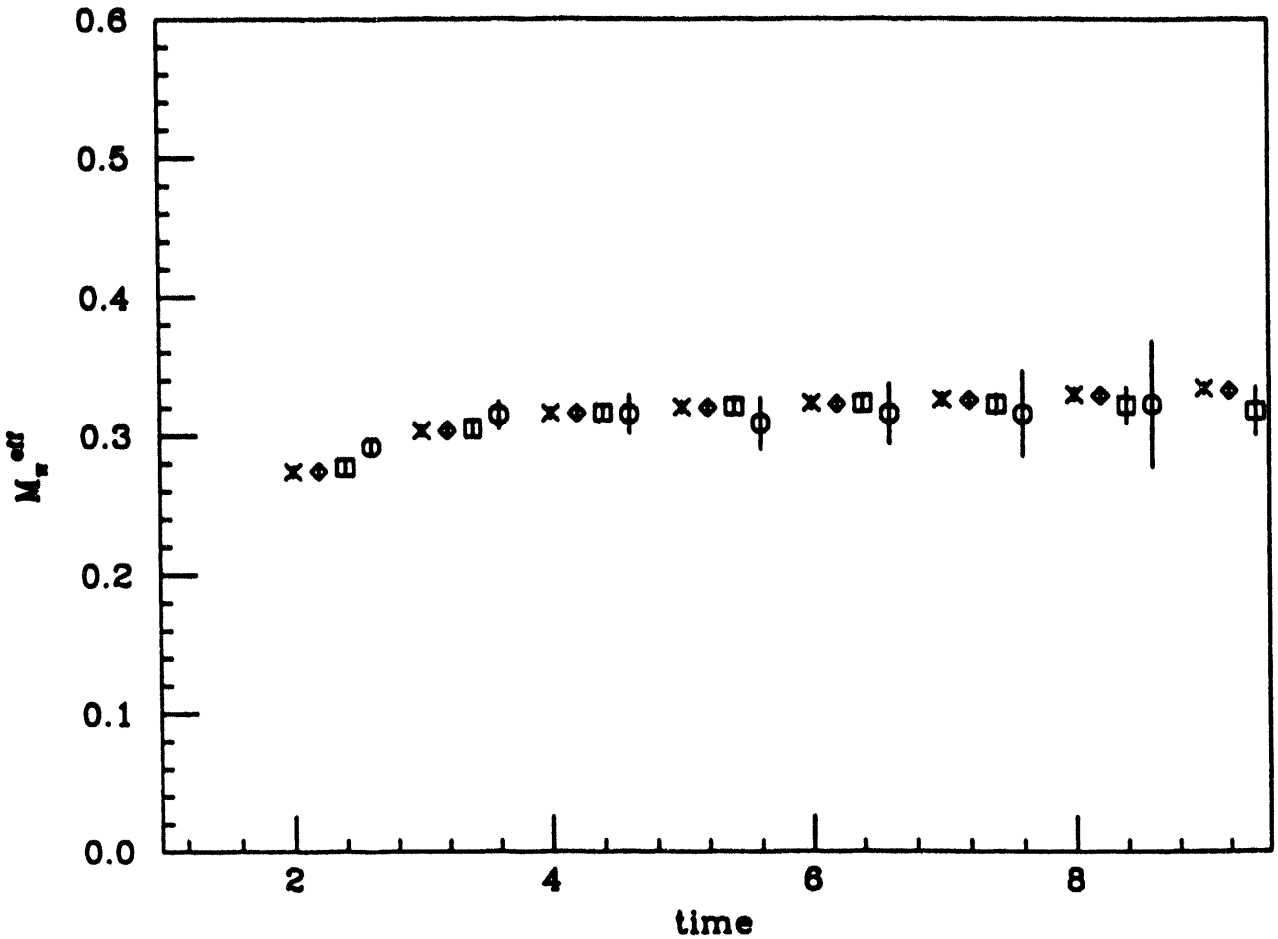

Fig. 9

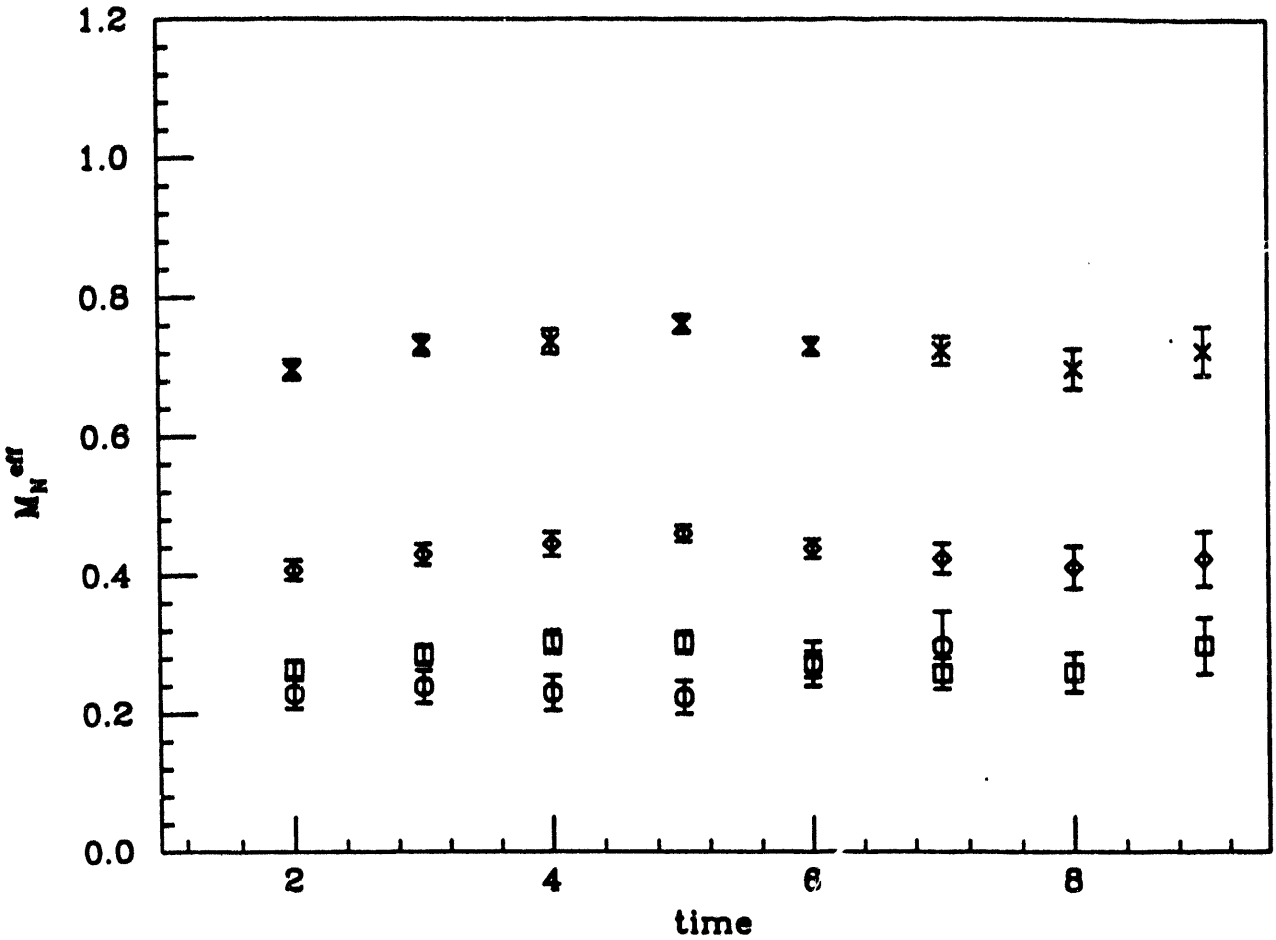

Fig. 10

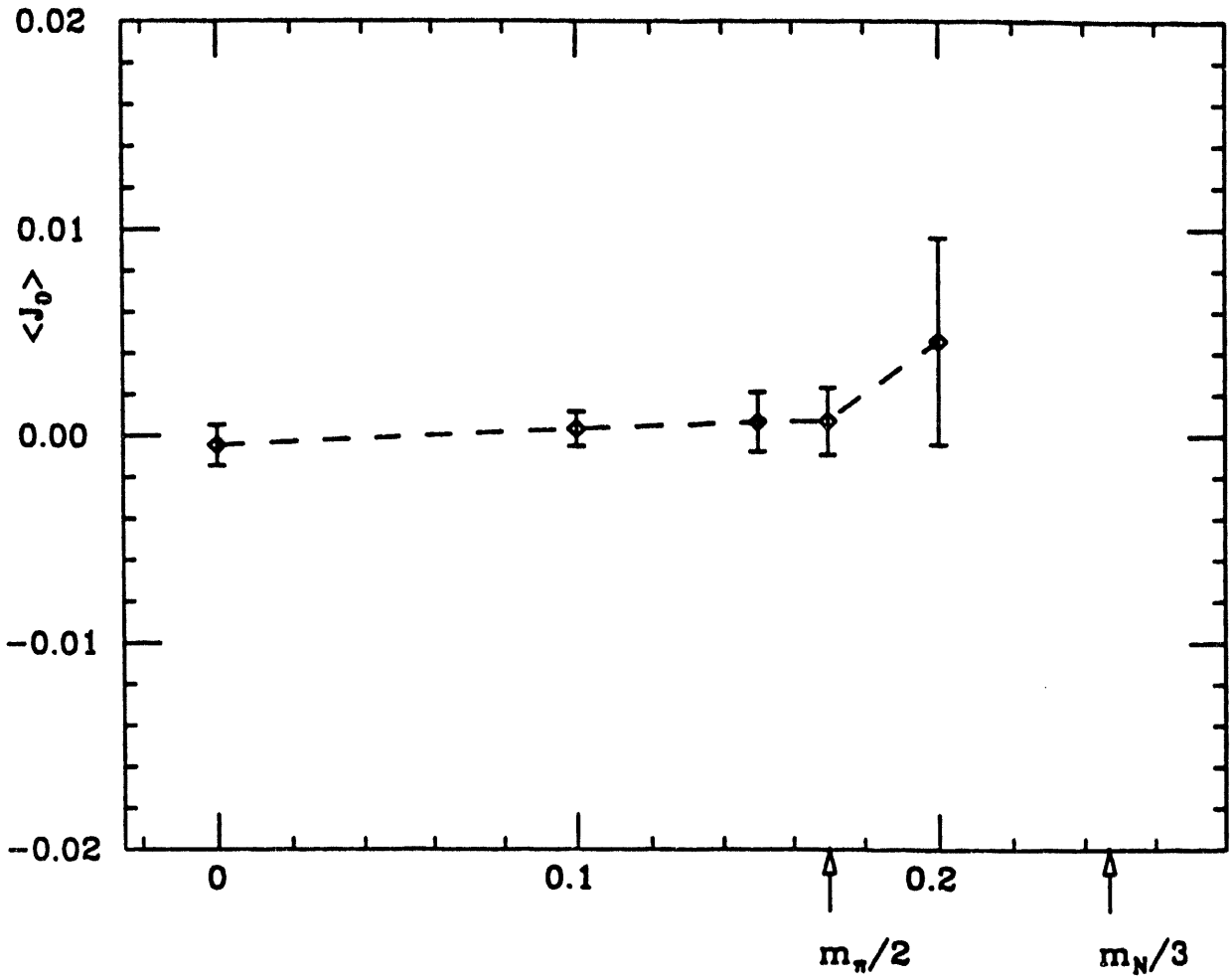

Fig. 11a

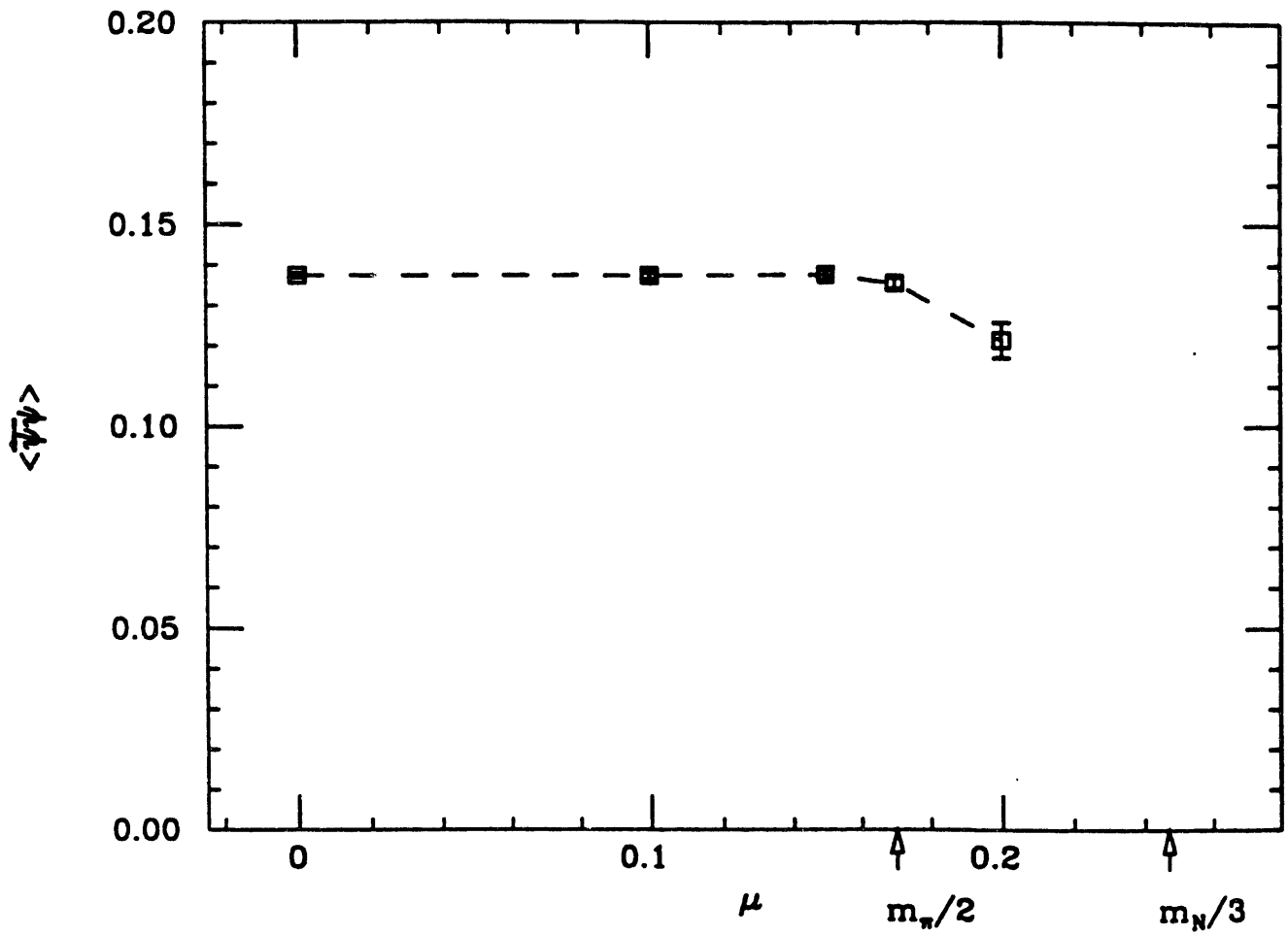

Fig. 11b

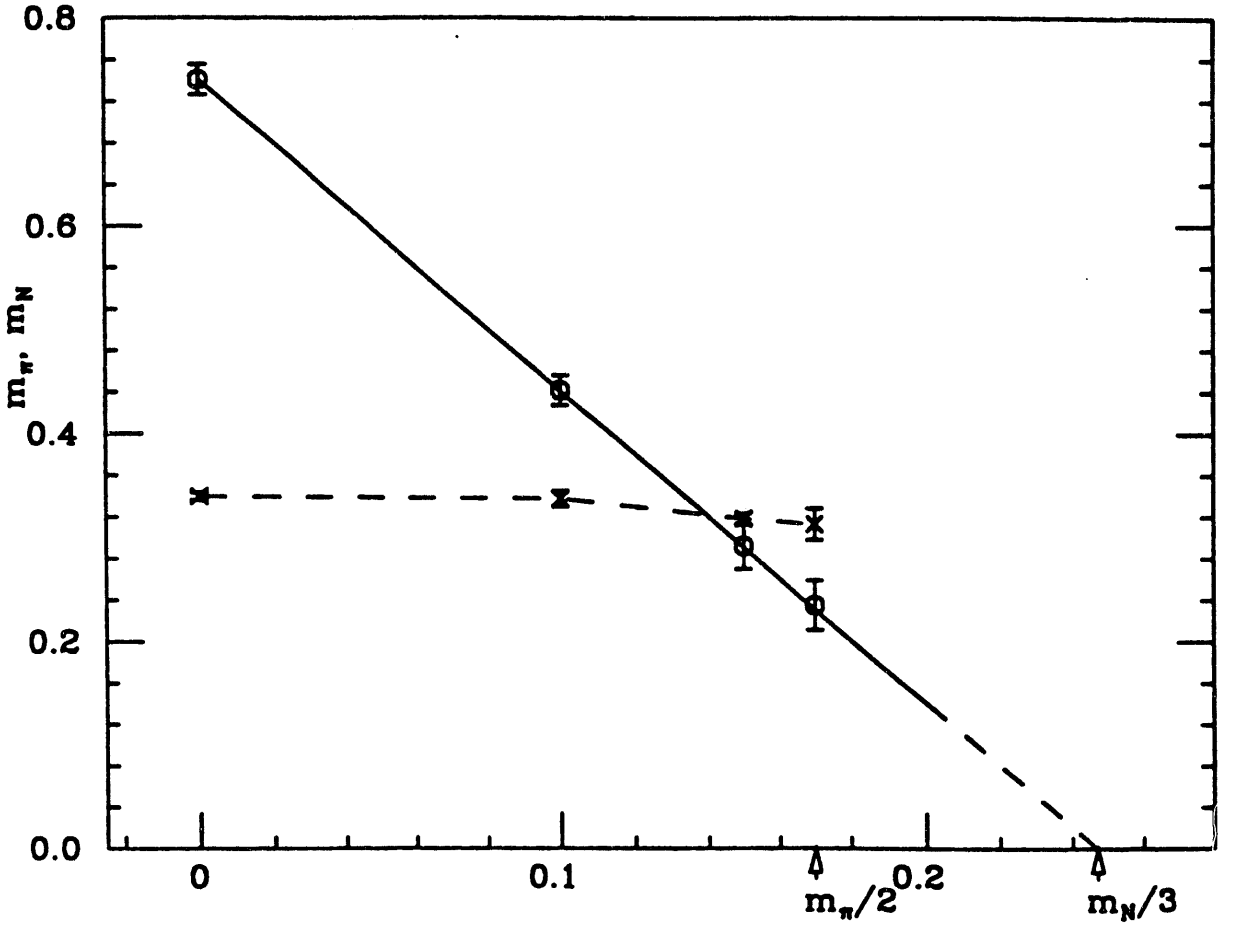

Fig. 12

DATE
FILMED
6/14/94

END